Design and construction of a 10 kW sorption heat pump prototype

Xavier Daguenet-Frick, Paul Gantenbein, Patrick Persdorf and Andreas Haeberle

Institute for solar technology SPF, University of applied science Rapperswil, Rapperswil (Switzerland)

Abstract

The cooling power of a closed adsorption system is depending on the thermo-physical properties of the sorbent/sorbate material combination. A good adaption by synthetic measures of the material properties to the temperature levels and mass flow rates of the external heating and cooling hydraulic loops has to be done consequently. Based on experimental results gained on a single vacuum chamber 1 kW average cooling power closed adsorption-desorption laboratory test rig, a scale-up to a four chamber 10 kW cooling power demonstrator was carried out. This scaling comprised the water sorbate evaporator and water vapour condenser design and the two combined fin-tube fixed sorbent bed adsorber/desorber heat and mass transfer units. The heat transfer fluid mass flow rates from the external heat sources and heat sinks was determined though simulation with an experimental results based model and is described for the mid temperature loop. In this paper, the design of the 10 kW prototype is described and technical decisions that were done as well as component choices are documented.

Keywords: sorption, thermally driven heat pump, cooling

1. Introduction

In solid adsorption heat pump systems, solar thermal energy or waste heat can be used for the sorbate desorption, enabling significant saving of CO_2 emissions. For the design of such heat pumps, the challenge is - like in all thermo-physical processes - the scale up from the experimental W (Watt) power range to the application kW power range. The aim of the presented work was to design a 10 kW adsorption cooling machine using in a first step Fuji Silica Gel RD-Type sorbent in a fixed bed arrangement and water as a sorbate. In a further step it is planned to replace the Fuji Silica Gel and use any other available sorbent materials (Aristov, 2014) – coatings or fixed bed etc. - as an alternative in the same machine.

The designed heat pump is based on a four chambers concept, comprising two Adsorption/Desorption (A/D) units as well as an evaporator (E) and a condenser (C) unit enabling a quasi-continuous operation (Ruch and Ammann, 2016). Fig. 1 shows a cross section view of the four chambers heat pump depicting two working phases.

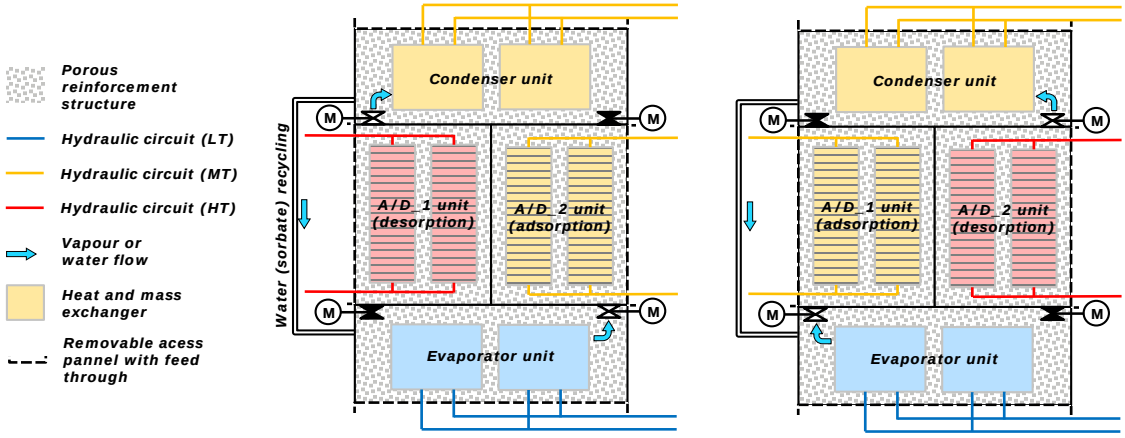

Fig. 1: Schematic of the 10 kW thermally driven Adsorption Heat Pump (AdHP) comprising Adsorber-Desorber heat exchangers (A/D 1 & A/D 2) and the Evaporator and Condenser units.

On this schematic, internal controlled vapour valves as well as the liquid water recycling drain back tube are also depicted. The sorbate flow direction as vapour (upward arrows) and as liquid (downward arrows) is shown in the figure 1.

doi:10.18086/eurosun2018.04.11 Available at http://proceedings.ises.org

A quasi continuous operation of the adsorption machine is reached though switching the motor (M in the figure) driven vapour valves and the temperature levels in the A/D units from high (desorption) to mid (adsorption) and vice versa. For a good performance optimized temperature differences from the units – A/D, condenser and evaporator – to the heat transfer fluid in the external loops and their flow rates are essential. In the following sections 2.1 the characterization of the sorbate immersed evaporator by determining the location of the onset of evaporation is described. The section 2.2 describes the A/D design. In section 2.3 the mid temperature loop flow rate modelling is shown. After power scaling considerations in this section 2 section 3 comprises the design and manufacturing of the sorption heat pump.

2. Experimental based modelling

Design of the 10 kW prototype is based on modelling results. To establish the models, experimental measurement campaigns were carried out on both E/C as well as A/D heat and mass exchangers.

2.1. Preliminary characterisation of one E/C heat and mass exchanger

For the E/C heat and mass exchanger, the first investigations were focused on the localization of the nucleation sites on the evaporator (limiting element). The experimental setup consists in two spiral heat and mass exchangers depicted on Fig. 10 (one used as evaporator, the other as condenser) placed in glassed containers and linked together on one side with a butterfly valve (vapour feed through) and on the other side by a small flexible tube (ID = 6 mm) shaped in a siphon (condensate return flow). Temperature and mass flow of both Heat Transfer Fluid (HTF) loops flowing respectively through the evaporator and the condenser can be controlled and measured. Incondensable gases were removed from the vacuum tight containers so that only water in equilibrium with its vapor is present round the heat and mass exchangers.

Imaging of the evaporator was carried out for four water levels (H, in mm) and several temperature differences between HTF inlet of the evaporator and condenser. One of the post treated image is presented on Fig. 2, left. On this figure, the warm colours betrays the high reflection areas (mainly linked with the presence of vapour bubbles). According to the graph presented on the right of Fig. 2, nucleation occurs on the entire heat exchanger height only by strong temperature differences (i.e. overheating). Furthermore, when the evaporator is not completely immersed, splashes issued from the vapour bubbles are wetting the tubes above leading to the formation of a film and an evaporation at the pressure of the evaporator chamber (limited overheating required).

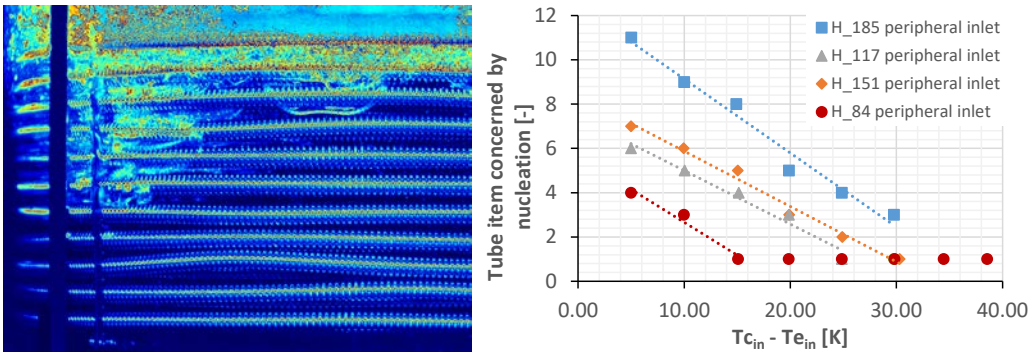

Fig. 2: Localization of the nucleation sites on the Evaporator in warm colours (posttreatment of a set of 1000 images @ 2 Hz, 7.5 ms exposure time) ΔT = 25 K, ΔP = 9.5 mbar, Q = 4300 W (left) and localisation of the nucleation depth for different water level in function of the temperature differences between HTF inlet of the evaporator and condenser (right).

Finally, it was found out that higher exchanged power were reached when the HTF inlet is placed in the centre of the exchanger. In fact, the HTF inlet matches with the most overheated area which also is the location where nucleation mainly occurs. Furthermore, the vapour bubbles originated at the centre of the heat exchanger have more probability to wet the overhanging tubes and to trigger further nucleation that the vapour bubbles at the periphery.

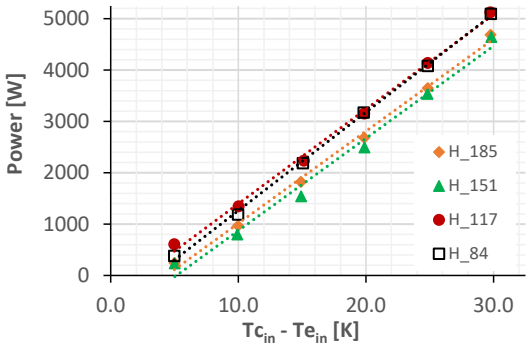

Fig. 3: Exchanged power for different water levels in the evaporator in function of the temperature differences between HTF inlet of the evaporator and condenser.

According to the results presented on Fig. 3, the evaporator is working in the best conditions when less than half immersed. Furthermore, up to 10 kW of heat was exchanged on a single module (by a temperature difference of 50 K). For the evaporator unit of the 10 kW AdHP Prototype, this experimental measurement campaign has shown that the number of heat exchangers can be reduced from 6 to 5 modules.

2.2. A/D unit: adsorption-desorption measurement and results

For the upscaling of A/D heat and mass exchanger extended experimental measurements were carried out in a single vacuum chamber 1 kW cooling power setup (Gantenbein et al., 2017). This double jacket single chamber experimental facility can be equipped with an A/D module as well as a combined Evaporator/Condenser (E/C) module.

For the A/D geometrical design a cubic shaped 6.6 m^2 fin-tube all-aluminium adsorption-desorption module was used to carry solid sorbent beads (Freni et al., 2016), see Figure 4. This unit has a surface to volume ratio of 0.54 m^2/l. The vapour flow is towards the four sides of the cube (arrows in figure 4) while the front ends of the A/D are aluminium plates impermeable for water vapour. The A/D consists of 6 tube columns and 9 of these in parallel. Measurements with two fin pitches (s = 3 mm and 5 mm) were carried out, a fin thickness of 0.18 mm and a particle beads size d_p of 0.85 mm < d_p < 1.7 mm. The spherical shaped Fuji RD-Type Silica Gel particles filling amounts of 7.5 kg and 8.4 kg for the 3 mm and the 5 mm fin spacing A/D units were used, respectively.

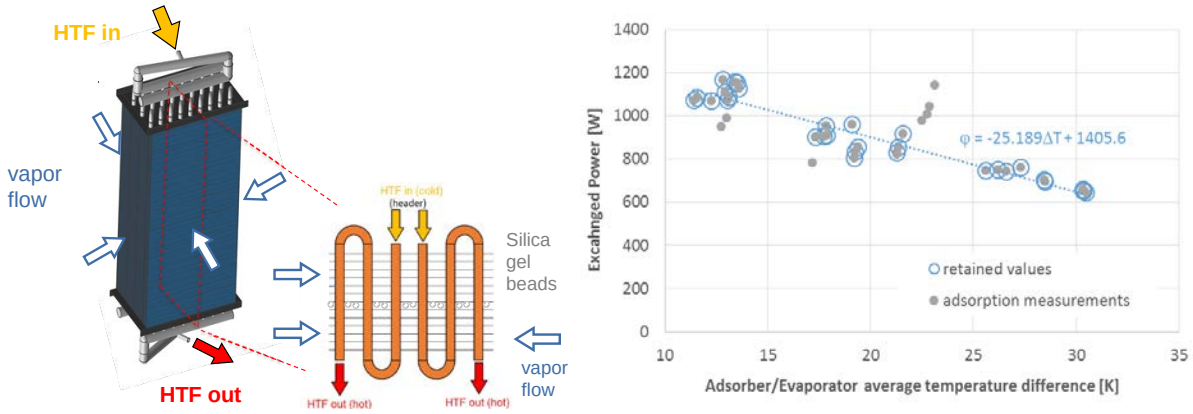

Fig. 4: 1 kW average A/D module installed in the single vacuum chamber with heat transfer fluid (HTF) flow direction in the adsorption mode and cross section view of the "crossed counter" current vapour and HTF flow A/D module (left); aggregated measurement data of time-averaged power measurements for the adsorption process (right).

Measurements were achieved with external fluid loop temperatures in the range of 30 to 50 °C for the adsorption process (mid temperature loop) and between 70 and 95 °C for the desorption process (high temperature loop), while adsorption and desorption cycle length t_c from 900 s up to 3600 s were performed. The peak cooling power reached values up to 2.2 kW. Figure 4 (right) shows power measurement time averaged results (t_c = 900 s) for the evaporation/adsorption (E/A) process in function of the average heat transfer fluid (HTF) temperature difference in the adsorber and in the evaporator. Similar measurement data post processing was carried out for the Desorbtion/Condensation (D/C) processes.

Based on the experimental measurements with A/D heat and mass exchangers of different fin spacing, a numerical model (Daguenet-Frick et al., 2017) was defined to assess the heat pump behaviour depending on the boundary conditions, i.e. temperature levels of the external heat sources and sinks and the mass flow rates (power) in the hydraulic loops. This model includes pumping power (in function of pressure drop) calculations in the external heat transfer fluid loops. Based on the results, a parallel hydraulic connection of the adsorption unit(s) and condenser unit is advantageous, see next section. A fin spacing of 3.0 mm should be preferred for the A/D heat and mass exchangers. An optimized heat transfer fluid (HTF) mass flow rate was also determinate.

Focusing on a 10 kW cooling power machine, the scale up task was carried out in two steps. As a first step from the lab setup of 1 kW to 1.6 kW, a linear increase of the A/D length was defined, keeping its cubic structure. For the further upscaling (reaching the power of 10 kW), a hydraulic parallel arrangement of 6 such A/D modules was designed and manufactured.

2.3. A/D unit: external fluid loop modelling and upscaling

Temperature levels as well as volume flow rate of the three external fluid loop are defining the 10 kW adsorption heat pump boundary conditions. Based on the linear approximation of the power in function of the temperature differences for both E/A and D/C processes (see paragraph above), a numerical model was set up. Calculations are done in steady state and an ideal efficiency of the machine is assumed (i.e. the power transferred during E/A and D/C processes are identical). Based on the temperature boundary conditions, the heat transfer are calculated by the model for the E/A process and defines the power exchanged for the D/C process as well as the output HTF temperatures. Looping stops as soon as no significant power variation are noticed. For the medium temperature source HTF loop two configurations are investigated: adsorber module hydraulically connected either in serial or in parallel with the condenser unit. For the HTF loops, pressure drop as well as pumping power are calculated. Figure 5 shows some results of a parametrical study carried out on the external fluid loops. According to simulation, a volume flow rate higher 2.4 m^3/h will dramatically increase the pumping power with only a minor increase of the heat exchanged. At this volume flow rate, a serial connection (--) of the A (A/D in adsorption) and C (condenser) units will enhance the heat $\Phi_{a,--}$ exchanged by 3% but with 39 % higher pumping power $W_{pp,--}$ compared to $W_{pp,//}$ in a parallel connection. Figure 5 shows that using 3 mm fin spacing increases the exchanged power (+ 6% in comparison to the 5 mm spacing) and that a theoretical minimal pumping power W_{pp} is reached for a distribution ratio of 0.57 (flow rate A to flow rate C).

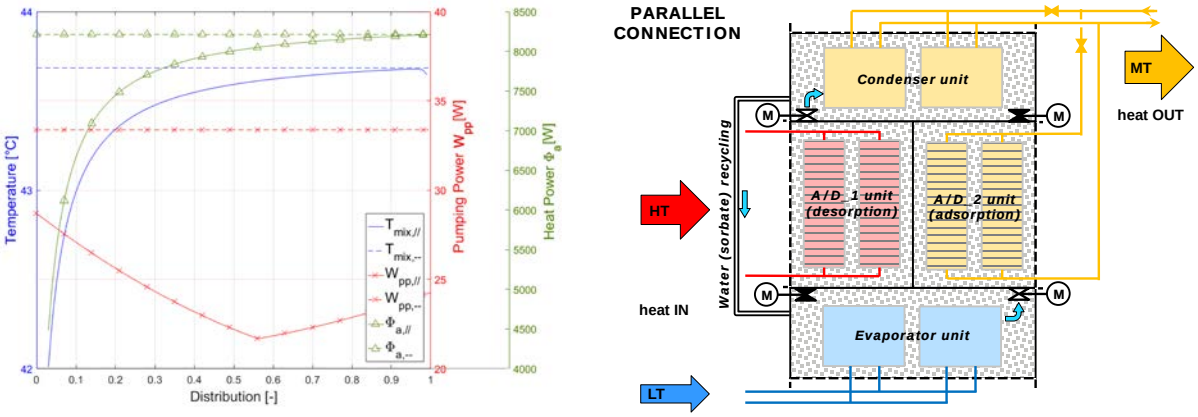

Fig. 5: Temperature at the outlet of the mid temperature HTF loop ($T_{mix,}$ //, $T_{mix,}$ --), pumping power ($W_{pp,//}$, $W_{pp,--}$) and heat power exchanged ($\Phi_{a,//}$, $\Phi_{a,--}$) by the adsorber depending on the distribution factor for a 3 mm and 5 mm fin spacing (left); A and C units connected in parallel (right).

3. Heat pump design and construction

3.1. General design

For the design of the heat pump, a mechanically self-supported concept was retained (cf. Fig. 6); the thin stainless steel envelop insuring the vacuum tightness is indirectly supported by the heat and mass exchangers. Below this welded container envelop, reinforcement walls (in grey on Fig. 6) are foreseen to equalize the mechanical constrains. This structure as well as the ceramic foam (in white) placed between the heat and mass exchangers are porous in order to distribute the sorbate vapour flow to the heat exchangers modules (in blue for the condenser

unit and in red for the A/D units). The first generation A/D modules are using silica gel beads placed in a fin-tube all-aluminium heat exchanger whereas the E and C modules are based on spiral coiled stainless steel corrugated tubes.

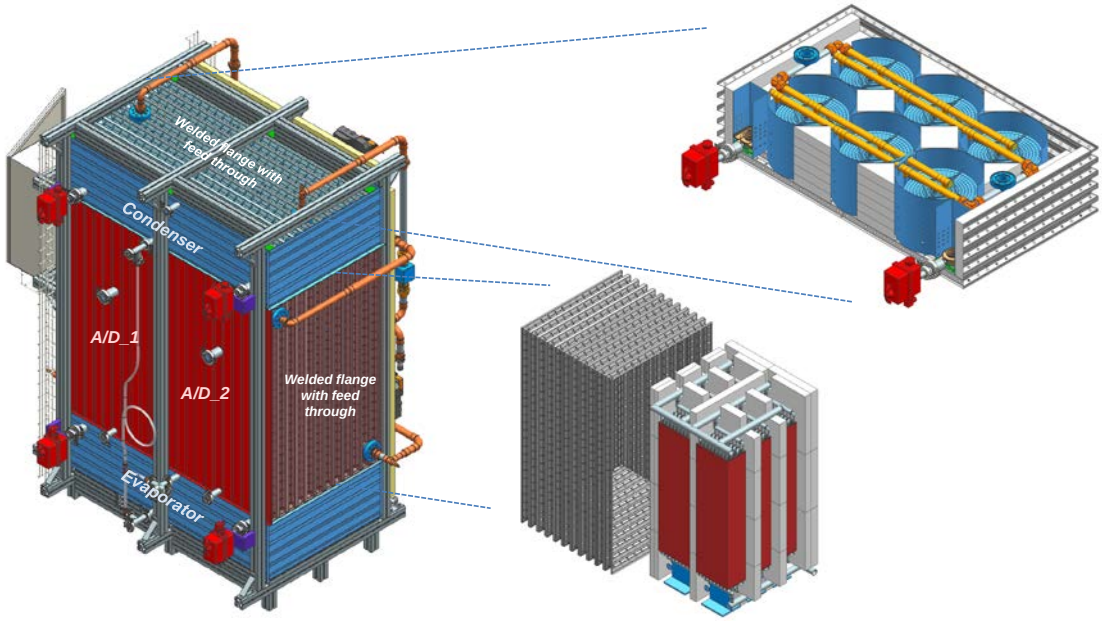

Fig. 6: CAD view of the four chamber adsorption heat pump with exploded view of the Condenser unit (top right) and of an A/D unit (bottom right).

Aiming to test a second generation of optimized sorbent, the whole concept is based on dismountable welded flanges (depicted on Fig. 6) enabling to replace the A/D heat and mass exchanger units.

3.2. AdHP hydraulics & connections

For the case of a replacement of the A/D heat and mass exchanger units, dismountable feed through have been in-house designed, manufactured and vacuum leakage tested (see Fig. 7). These feed through have to ensure tightness on the heat transfer fluid loop side as well as on the container side (vacuum) and allow to remove the door prior to the heat and mass heat exchanger replacement.

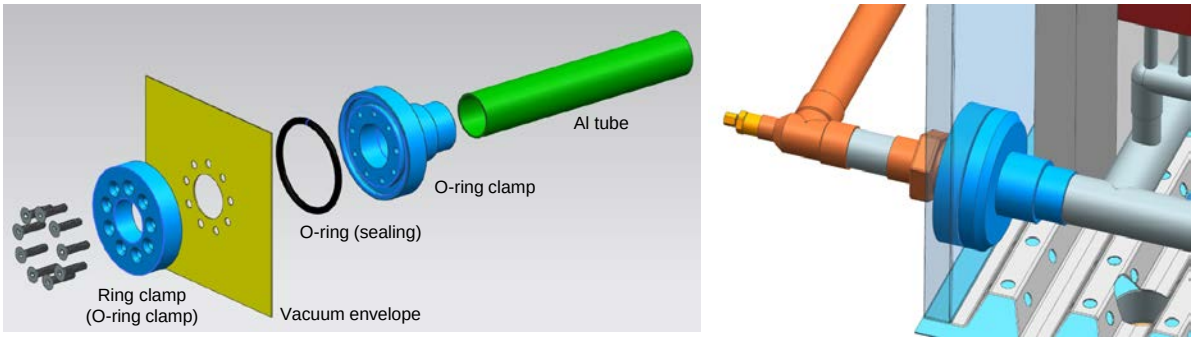

Fig. 7: CAD view of the feed-through exploded (left) and assembly connected to the AD unit (right).

The rear side of the AdHP (shown on Fig. 8) is constituted of a panel comprising tubing, motorised valves and magnetic inductive flow sensors as well as temperature sensors. These motorised valves are ensuring the distribution of the heat transfer fluid between the three heat sources/sinks (see Fig. 1) and the four heat and mass exchangers. The fluid distribution factor between the condenser and the absorber (see paragraph 2.3) can be controlled and optimised. This panel also includes a fluid pump ensuring heat recovery between the two A/D units (from regenerated and hot desorber to the saturated absorber). A heat recovery mode (depicted on Fig. 9) can be activated between each adsorption/desorption cycling.

Fig. 8: AdHP rear side: tubing and connecting interfaces to the internal components; heat recovery pump (CAD left, real facility right).

Fig. 9 shows the Graphical User Interface (GUI) of the National Instruments LabVIEW® Software. Thanks to this interface, different machine internal measured values like temperature, mass flow rate and pressure inside of the AdHP chambers can be measured and stored to analyse and assess the operation of the machine.

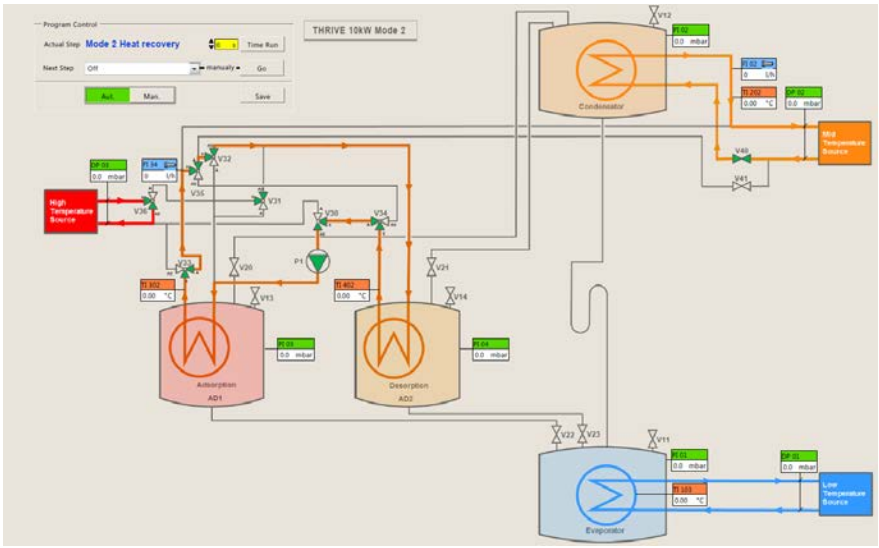

Fig. 9: Graphical User Interface (GUI) of the AdHP; heat recovery mode.

Self-learning PID modulators are implemented to control the flow distribution in the Medium Temperature (MT) loop. A control of the adsorption/desorption cycle length either with a timer or on the basis of a pressure differences measurement or heat power calculation is foreseen.

3.3. E/C design and manufacturing

As shown on Fig. 6, an evaporator and a condenser unit are implemented in the AdHP prototype. These units are made of spiral formed heat and mass exchanger modules, modules themselves constituted of eleven coiled corrugated stainless-steal hoses. These corrugated tubes are in parallel connected to copper inlet and outlet manifolds which are designed and hydraulic configured in Tichelmann arrangement (see Fig. 10, left).

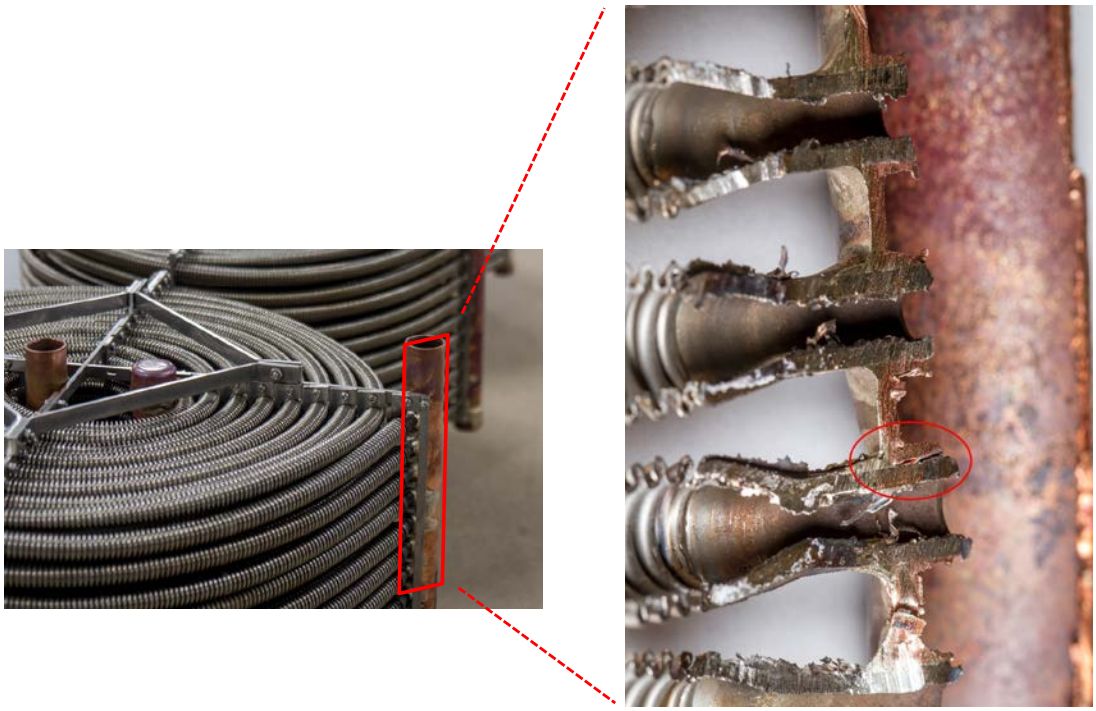

Fig. 10: E/C spiral heat and mass exchanger module (left) and cut of its manifold showing the copper/stainless-steal junction with one crack (right).

Considerable mechanical stability issues (spring effect of the tubes) were experienced on the copper / stainless steel junction. They were evidenced during the leakage tests each part was submitted prior to implementation in the 10 kW AdHP prototype. One heat and mass exchanger had to be sacrificed (see manifold cut shown on Fig. 10, right) in order to find out the origin of the leakages and thus for an improvement of the soldering/brazing process.

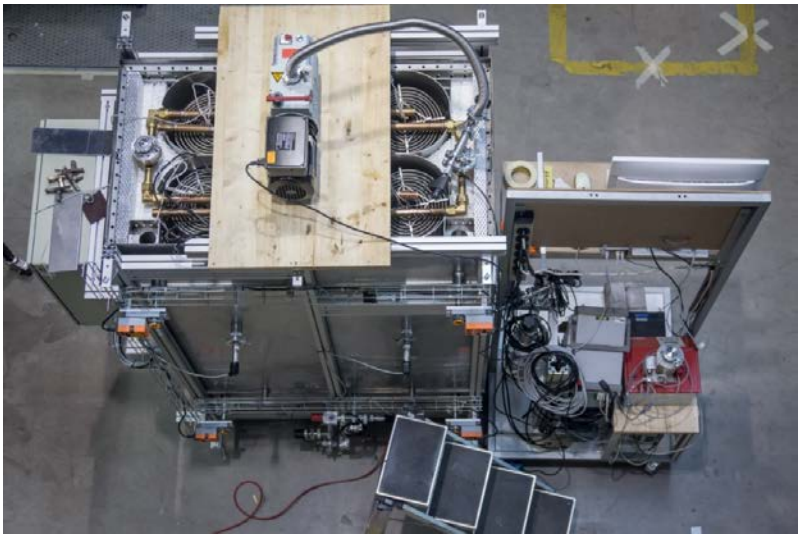

Fig. 11: Implementation of the condenser heat and mass exchanger unit in the container and leakage test (generally performed by pressure increase followed by a Helium leakage test with mass spectrometer).

Fig. 11 shows the top of the AdHP prototype with implemented condenser unit during a leakage test. This picture was taken before the implementation and welding of the container top wall.

3.4. A/D manufacturing

In the same way as the E and C units, two A/D units were implemented in the AdHP prototype (see Fig. 6). On Fig. 12, one of these two units is shown before (left) and during (right) the implementation into the container (arrow). On this last picture, the white porous ceramic foam enabling the assembly to be mechanically self-supported can be seen.

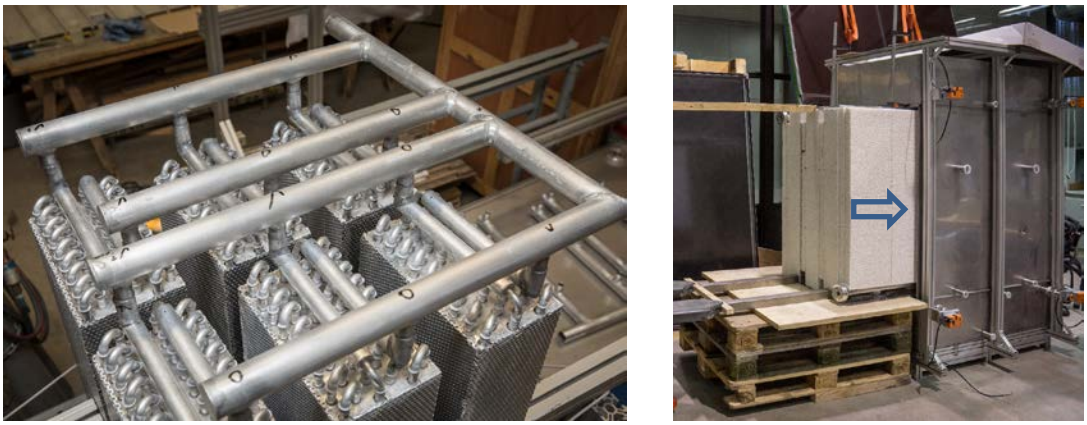

Fig. 12: All-aluminium A/D 10 kW module with brazed manifold (left), dragging of the AD1 into the vacuum envelope (right).

4. Outlook

The sorption heat pump demonstrator is set up and Helium leakage tests were performed. An assessment through measurements of the machine with A/D containing Fuji Silica Gel RD-Type is planned. Further measurements with fixed sorbent bed or coated A/D or any other structure of the sorbent can be performed. The improvement of the evaporator and the condenser is planned.

5. Acknowledgements

The funding by the Swiss National Science Foundation SNSF in the frame of the National Research Program NRP 70 and by the University of Applied Sciences Rapperswil is highly acknowledged. Franz Steiner and Albert Trudel, supporting engineers, are also gratefully acknowledged.

6. References

Aristov Y., 2014. Concept of adsorbent optimal for adsorption cooling/heating. Applied Thermal Engineering 72, pp. 166-175, doi: 10.1016/j.applthermaleng.2014.04.077.

Ruch, P., Ammann, J., 2016. Materials and System design for adsorption heat pumps. 12th International Conference on the Fundamentals of Adsorption, Friedrichshafen Germany.

Daguenet-Frick, X., Moullet, Y., Gantenbein, P., Persdorf, P. and Notter, D., 2017. Adsorption heat pump upscaling from 1 kW to 10 kW of cooling power: experimental based modelling, International Sorption Heat Pump Conference, Tokyo Japan.

Gantenbein, P., Daguenet-Frick, X., Bont, F., Persdorf, P. and Notter, D., 2017. Cooling power determination by measuring the adsorbed vapour mass variations, International Sorption Heat Pump Conference, Tokyo Japan.

A. Freni, G. Maggio, A. Sapienza, A. Frazzica, G. Restuccia, S. Vasta, 2016. Comparative analysis of promising adsorbent/adsorbate pairs for adsorptive heat pumping, air conditioning and refrigeration. Applied Thermal Engineering 104, pp. 85-95, doi: 10.1007/s40243-018-0131-y.